



...Dedicated to my family
Deuta, Maa, Bai & Dada-Bou



PREFACE

The research work presented in the thesis, including survey of literature, identifying the research gap, conducting the experiments, data interpretation, preparation of manuscripts and conference presentations are carried out by Miss Suranjana Patowary under the supervision of Dr. Pankaj Bharali in the Department of Chemical Sciences, Tezpur University.

The following publications and presentations are developed from the work presented in this thesis.

Parts of Chapter 1 are published as one review article and one book chapter:

1. **Patowary, S.**, Chetry, R., Goswami, C., Chutia, B., and Bharali, P. Oxygen reduction reaction catalysed by supported nanoparticles: advancements and challenges. *ChemCatChem*, 14(7):202101472, 2022.
2. **Patowary, S.**, Chutia, B., Hazarika, K. K., and Bharali, P. Hybrid electrocatalysts with oxide/oxide and oxide/hydroxide interfaces for oxygen electrode reactions. In: *Heterogeneous Nanocatalysis for Energy and Environmental Sustainability*. Vol 1; 2022:111-132.

A version of Chapter 3 is under preparation for publication:

1. **Patowary, S.**, and Bharali, P. A systematic study of non-PGM metal hydroxides/oxides toward oxygen electrocatalysis (**Manuscript under preparation**).

A version of Chapter 4 is published as a journal article and is presented in two conferences:

1. **Patowary, S.**, Watson, A., Chetry, R., Sudarsanam, P., Russell, A. E. and Bharali, P. Oxygen-Vacancy Rich $\text{Co}_3\text{O}_4/\text{CeO}_2$ Interface for Enhanced Oxygen Reduction and Evolution Reactions. *ChemCatChem*, 17(6): 202401759, 2024.
2. **Oral presentation**, CeO_2 -modified Oxygen Vacancy-rich Co_3O_4 on Graphene Nanoplatelets for Enhanced Oxygen Reduction and Evolution Reaction, “*SusChemE 2.0*” at ICT, Mumbai, from September 14 - 16, 2023.

3. **Poster presentation**, Graphene nanoplatelet supported $\text{Co}_3\text{O}_4@\text{CeO}_2$ as bifunctional electrocatalyst for oxygen reduction and evolution reactions in alkaline media, “*Electrochem2022*” at The University of Edinburgh, Scotland, from September 4–6, 2022.

A version of Chapter 5 has been presented in a conference and another version of it has been submitted to a peer-reviewed journal:

1. **Poster presentation**, A robust bifunctional $\text{Co}_3\text{O}_4\text{--CeO}_2$ electrocatalyst with crystalline-amorphous interfaces toward ORR and OER, ‘*SusChemHeca*’ at Tezpur University, Tezpur, from March 14–15, 2024.
2. **Patowary, S.**, Chutia, B., Gogoi, P. M. and Bharali, P. A robust bifunctional $\text{Co}_3\text{O}_4/\text{Co}_x\text{Ce}_{1-x}\text{O}_{2-\delta}/\text{C}$ electrocatalyst with crystalline-amorphous interfaces toward ORR and OER (**Manuscript submitted**).

A version of Chapter 6 is under preparation for publication:

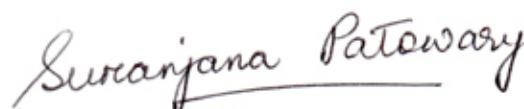
1. **Patowary, S.**, Watson, A., Bhattu, S., Sudarsanam, P. Russell, A. E., and Bharali, P. Simple hydrothermal route to synthesize $\text{CoO}_x(\text{OH})_y/\text{CeO}_2/\text{C}$ hybrid for enhanced oxygen reduction and evolution reaction (**Manuscript under preparation**).

DECLARATION

This thesis entitled “**Design of Hybrid Electrocatalysts with Oxide-Oxide/Hydroxide Interfaces**” being submitted to the Department of Chemical Sciences, Tezpur University, is a presentation of the original research work carried out by me. Any contribution (texts, figures, results or designs) of others, wherever involved, is appropriately referenced in order to give credit to the original author(s). All sources of assistance have been duly acknowledged. I affirm that neither this work as a whole nor a part of it has been submitted to any other university or institute for any other degree, diploma or award.

Date: 07-04-2025

Place: Tezpur



(Suranjana Patowary)



TEZPUR UNIVERSITY

(A Central University)

Napaam, Tezpur – 784 028, INDIA

Tel (O): +91-3712-275064

Fax: (O): +91-3712-267005/6

E-mail: pankajb@tezu.ernet.in

Website: www.tezu.ernet.in

Dr. Pankaj Bharali

Associate Professor

Department of Chemical Sciences

Certificate from the supervisor

This is to certify that the thesis entitled “**Design of Hybrid Electrocatalysts with Oxide-Oxide/Hydroxide Interfaces**” submitted to the School of Sciences, Tezpur University in part fulfilment for the award of the degree of Doctor of Philosophy in Chemical Sciences is a record of research work carried out by **Miss Suranjana Patowary** under my supervision and guidance. The chapters 4 and 6 of the thesis titled “*CeO₂-mediated oxygen vacancy rich Co₃O₄ on graphene for enhanced oxygen reduction and evolution reaction in alkaline media*” and “*Simple hydrothermal route to synthesize CoO_x(OH)_y/CeO₂/C hybrid for enhanced oxygen reduction and evolution reactions*” respectively, involves the work done by Miss Suranjana Patowary in collaboration with Prof. Andrea E. Russell, University of Southampton, Southampton, United Kingdom under Commonwealth Split-site Scholarship 2021. All help received by her from various sources have been duly acknowledged. No part of this thesis has been submitted elsewhere for award of any other degree.

Dr. Pankaj Bharali

Designation: Associate Professor

School: Sciences

Department: Chemical Sciences

Date: 07-04-2025

Place: Tezpur

ACKNOWLEDGEMENT

As I pen down these words, my heart is filled with immense gratitude and contentment. I feel humbled and fortunate to experience this wonderful journey of research. First and foremost, I express immense gratitude to the Almighty for giving me the opportunity to walk the path of knowledge. This thesis would not have been possible without the collective efforts of the following.

At the outset, I would like to thank my supervisor Dr. Pankaj Bharali for his sincere guidance, relentless support and suggestions throughout the journey. I am immensely grateful to him for making me a part of his research group. I express my sincere gratitude to Prof. Andrea E. Russell for giving me a place in her lab and for being my host-supervisor at University of Southampton, United Kingdom (Period March 2022 to March 2023). I shall be forever grateful for her continued guidance in my research work. I am thankful to both the supervisors for their combined efforts in making me grow as a researcher. From them, I have learnt many key aspects of academia (professionalism, accountability of work, proper journaling of data, academic networking, scientific writing, teamwork, etc.).

I would like to thank the doctoral committee members, Prof. Nashreen S. Islam and Prof. Utpal Bora for their time-to-time supervision on my research progress. Without their inspiration and recommendations, I would not have achieved this milestone.

I am thankful to honourable Vice-Chancellors Prof. Shambhu Nath Singh (current) and Prof. Vinod Kr. Jain (former) of Tezpur University for providing all the infrastructures during my tenure. I am thankful to the Head of Department Prof. Panchanan Puzari (present), Prof. Ruli Borah (former) and Prof. Ashim J. Thakur (former) for their support in smooth conduct of the research work.

I am thankful to all teaching and non-teaching staff of the Department of Chemical Sciences, Tezpur University and the School of Chemistry, University of Southampton for their support in smoothly conducting the research activities.

I acknowledge SAIC-Tezpur University, SAIJ-North-Eastern Hill University, CIF-IIT Guwahati, NCL-Pune, AMRC-IIT Mandi for providing sophisticated instrumental facilities. I would like to thank Dr. Putla Sudarsanam from IIT Hyderabad and Prof. Yusuke Yamada from Osaka Metropolitan University, Japan for providing me a chance to work with them.

I am deeply thankful to all the funding agencies without whose support this thesis work could not have been completed. I thank Tezpur University for non-NET institutional fellowship and Research Innovation Grant (TU-RIG, Memo No. DoRD/RIG/10-73/1592-A) and Department of Science & Technology (DST), Govt. of India for DST-SERB project (CRG/2023/008294). I acknowledge University of Southampton for research support (UID33939918). I thank the Commonwealth Scholarship Commission (CSC, UK) and the Foreign, Commonwealth & Development Office (FCDO), London for commonwealth split-site scholarships. I acknowledge Diamond Light Source, Oxford for providing synchrotron facilities for my research (Experiment No. SP29271-5).

I would like to thank Prof. Guy Denuault and Prof. Peter Wells from the Southampton Electrochemistry Group for their help and support. I fondly remember and express my deep gratitude to Connor Sherwin, Amber Watson, Dr. Oliver Blackman, Nickolay Zhelev, Dr. Khaled Mohammed, Dr. Thomas Wakelin, Dr. Shibin Thomas, Dr. Jagriti Sethi from the Southampton Electrochemistry Group for always helping me to learn. I will always cherish the brainstorming discussions I had with them. I would like to acknowledge Mr. Lee R Mulholland of University of Southampton for making, fixing and safe shipping all my glass wares

from UK to India. I express my love and gratitude to Mrs. Selina Denuault, Geny, Fernanda Muñoz-Salazar and Wangke Yu for making my stay at Southampton, England joyful.

I would like to thank all my teachers from school till university for their relentless efforts in making me who I am today; special mention goes to Jeevan Sir and Pawan Sir.

I greatly appreciate the love and support from the entire research scholar fraternity of Department of Chemical Sciences, Tezpur University. I would like to mention Dr. Chiranjita Goswami, Dr. Kumar K. Hazarika, Dr. Bhugendra Chutia, Dr. Biraj J. Borah, Shaheen P. Bhuyan, Bhrigu Kumar Pegu, Pragya Moni Gogoi and Darshan Jyoti Gogoi for their assistance, love and support throughout the thesis work. Special mention goes to my partner Rahul and my confidants Sangeeta, Protima, Kakoli & Rimpi Sarma for their unwavering support and belief in my capabilities. I am deeply grateful towards my friends Shilpa Neog, Annesha Kar, Pooja Mushahary, Priyanka Basumatary, Aliya Zesmina, Himanshu Sarma, Nayab Hussain, Pranamika Sarma, Dehabrat Pathak, Hiya Talukdar, Nobomi Borah, Bikash Ch. Mushahary, Raju Chouhan, Samiran Morang, Partha Pratim Churi, Rituparna Saikia, Kangkana Baruah, Sultana Parveen Ahmed & Dr. Asadulla Asraf Ali for their immense support throughout all these years. Friends Ashok Barhoi of IIT Patna and Mongoli Brahma of IIT Guwahati are acknowledged for helping me get some of the data used in the thesis work. I thank two of my project students Angana Mahanta and Priya Mehta for assisting me collect some of my data. I express my gratitude to Mrs. Luishlema Baruah and Pihu for their love and hospitality on every occasion throughout the years.

I express my humble gratitude towards the hostel dogs Goofy, Chumki, TimTim & TukTuk who added colors to my life.

I express my deepest gratitude to my family: Dr. Nityananda Patowary (Deuta), Dr. Mrs. Ela Rani Choudhury (Maa), Mrs. Jasoda Das (Bai), Mr. Madhurjya Patowary (Dada), Mrs. Leema Pathak (Bou), Mr. Uddipan Das (Dada) & nieces Chuku-Muku for being my 'Home'. I shall always remain indebted to them for their love, support and innumerable sacrifices for my well-being.

Lastly, I pray that I may always do justice to the doctorate degree! May I always give more than I take!

Thanking you,

Suranjana Patowary

LIST OF TABLES

Table	Title	Page No.
1.1	ORR mechanism	1-5
2.1	List of chemicals used	2-2
3A.1	Details of calculation of mass specific activities	3-10
3A.2	List of parameters in ECSA calculation.	3-11
3A.3	List of important electrocatalytic parameters- onset potential ($E_{\text{onset,ORR}}$), half wave potential ($E_{1/2}$), limiting current density (j_m), mass specific activity, ECSA, potential to reach 10 mA cm^{-2} of the catalysts towards ORR and ORR.	3-15
3B.1	Details of calculation of mass specific activities.	3-24
3B.2	List of important electrocatalytic parameters- onset potential ($E_{\text{onset,ORR}}$), half wave potential ($E_{1/2}$), limiting current density (j_m), mass specific activity, ECSA, potential to reach 10 mA cm^{-2} of the catalysts towards ORR and ORR.	3-29
4.1	BET surface area, pore width and pore volume of the catalysts.	4-6
4.2	Atomic wt.% in $\text{Co}_3\text{O}_4/\text{CeO}_2/\text{GNP}$ determined from ICP-OES.	4-6
4.3	Peak positions and relative % of Ce^{3+} and Ce^{4+} in Ce 3d XP spectra $\text{Co}_3\text{O}_4/\text{CeO}_2/\text{GNP}$.	4-10
4.4	Peak positions and relative % of Co^{2+} and Co^{3+} in Co 2p XP spectra of $\text{Co}_3\text{O}_4/\text{CeO}_2/\text{GNP}$ and $\text{Co}_3\text{O}_4/\text{GNP}$.	4-12
4.5	Summary of 1 st shell fitting of Co K-edge and the simulated parameters like Co-ordination number (N), Bond-length (R), Debye-Waller factor (σ^2), and inner potential shift (ϵ_o). R-factor represents goodness of fit.	4-15
4.6	The onset potentials ($E_{\text{onset,ORR}}$, $E_{\text{onset,OER}}$), geometric current densities for ORR at 0.6 V (j_{geo}), potential for 10 mA cm^{-2} for OER (j_{10}) are listed below.	4-23
4.7	Comparison of the performance recently reported Co_3O_4 -based electrocatalysts performance towards ORR/OER in 0.1 M KOH with our catalysts.	4-24
5.1	Average crystallite sizes as calculated from Scherrer equation.	5-4

5.2	Shifts in binding energies (B.E.) of Co 2p XPS spectra.	5-10
5.3	Evaluated electrocatalytic parameters of the as-synthesized catalysts and the benchmark Pt/C and RuO ₂ .	5-13
6.1	Atomic ratios of Co and Ce from ICP-OES.	6-5
6.2	Peak positions of Co 2p XP spectra in different catalysts and their shifts with respect to one another.	6-8
6.3	Peak positions and area integration ratios of Ce 3d XP spectra.	6-10
6.4	Summary of E _{onset,ORR} , E _{j10} , η and Tafel slopes of various ECs and RuO ₂ for OER derived from LSV curve at 1600 rpm.	6-22
7.1	A summary of all the catalysts synthesized in the thesis work and their catalytic performance indicators like onset potential for ORR (onset _{ORR}), half-wave potentials (E _{1/2}), limiting current density (j _{lim}), number of electrons transferred for ORR (n) and overpotential for OER (η_{10}).	7-6

LIST OF FIGURES

Figure	Title	Page No.
1.1	The anatomy of a typical hydrogen-based fuel cell.	1-3
1.2	Volcano plot for ORR.	1-4
1.3	A schematic of recent developments to Pt-based ECs.	1-6
1.4	(a–c, e, f) TEM and HRTEM images with distinguished lattice fringes, particle size distribution curve (inset image (a)), and (d) SAED pattern for the $\text{CuO}_x\text{–CeO}_2/\text{C}$ EC.	1-10
1.5	Scheme of the formation of the $\text{Mn}_3\text{O}_4@\text{CoMn}_2\text{O}_4$ and $\text{Mn}_3\text{O}_4@\text{CoMn}_2\text{O}_4\text{–Co}_x\text{O}_y$ nano-heterostructures when using either a cobalt chloride or a cobalt perchlorate solution. Green arrows in the bottom cartoon point at Co_xO_y nanocrystal nucleation sites.	1-11
1.6	(a) LSV, and (b) Tafel slopes (purple), resistance (dark cyan), and double-layer capacitances values (orange). ORR: (c) LSV, (d) LSV of $\text{NiO}/\text{NiCo}_2\text{O}_4$ nanofibers at different rpm, and (e) corresponding K–L plots of $\text{NiO}/\text{NiCo}_2\text{O}_4$ nanofibers. Inset: n values for ORR. (f) Bifunctional ORR/OER catalytic activity	1-12
1.7	Schematic illustration of the synthesis of four iron oxide or oxyhydroxide/GO composites	1-14
1.8	(A) CVs in N_2 - and O_2 -saturated, (B) LSV in O_2 -saturated 0.1 M KOH for NiFe-LDH , NiFe-LDH/GO and NiFe-LDH/rGO composites with 1600 rpm. (C) RDE voltammograms of rGO-LDH in O_2 -saturated 0.1 M KOH at a scan rate of 10 mV s^{-1} at different rotating speed, (D) the corresponding K-L plot of J^{-1} vs. $\omega^{-1/2}$. The inset shows the electron transfer number (n), and (E) RRDE voltammograms of NiFe-LDH/rGO in O_2 -saturated 0.1 M KOH. The disk potential is scanned at 10 mV s^{-1} and the ring potential is constant at 1.3 V. (F)	1-16

The electron transfer number n and percentage of HO_2^- at certain potentials are based on the corresponding RRDE results

1.9	(a) Different forms of carbon as catalyst-support (b) Raman spectra of GO, graphene, g-FePc, and pure FePc, (c) RDE measurements of oxygen reduction (negative current) and RRDE measurements of H_2O_2 oxidation (positive current) on g-FePc and Pt/C electrodes in O_2 -saturated 0.1 M KOH, (d) Comparison of ORR curves of FePc/C, g-FePc, FePc, and graphene in O_2 -saturated 0.1 M KOH at 1600 rpm, (e) Schematic illustration of the interaction between graphene and FePc and ORR process on g-FePc.	1-18
1.10	Schematic illustrating various defects and their respective features in crystals with multiple dimensions	1-19
2.1	Pictorial illustration of the synthesis of $\text{Co}_3\text{O}_4/\text{CeO}_2/\text{GNP}$.	2-4
2.2	Pictorial illustration of the synthesis of $\text{Co}_3\text{O}_4/\text{Co}_x\text{Ce}_{1-x}\text{O}_{2-\delta}/\text{C}$.	2-5
2.3	Pictorial illustration of the synthesis of $\text{CoO}_x(\text{OH})_y/\text{CeO}_2/\text{C}$.	2-6
2.4	(a) Diagrammatic illustration of Bragg's law, and (b) Diffraction peak and information content that can be extracted	2-7
2.5	A pictorial illustration of the 3-electrode setup and the potentiostat.	2-13
2.6	Typical CVs of Pt/C in N_2 - and O_2 -saturated 0.1M KOH taken at scan rate 10 mV s^{-1} .	2-15
3A.1	PXRD spectra of (a) $\text{Co}_3\text{O}_4/\text{GNP}$, (b) $\text{Ni}(\text{OH})_2/\text{GNP}$, and (c) CeO_2/GNP .	3-3
3A.2	FTIR spectra of (a) $\text{Co}_3\text{O}_4/\text{GNP}$, (b) $\text{Ni}(\text{OH})_2/\text{GNP}$, and (c) CeO_2/GNP .	3-4
3A.3	(a) Raman spectra, and (b) TGA of $\text{Co}_3\text{O}_4/\text{GNP}$,	3-6

	Ni(OH) ₂ /GNP and CeO ₂ /GNP.	
3A.4	EDX analysis of Co ₃ O ₄ /GNP; (a) the electron image (b) the EDX pattern, and (c-e) individual elemental maps for Co, O and C, respectively.	3-6
3A.5	EDX analysis of Ni(OH) ₂ /GNP; (a) the electron image (b) the EDX pattern, and (c-e) individual elemental maps for Ni, O and C, respectively.	3-7
3A.6	EDX analysis of CeO ₂ /GNP; (a) the electron image (b) the EDX pattern, and (c-e) individual elemental maps for Ce, O and C, respectively.	3-7
3A.7	CVs of (a) Co ₃ O ₄ /GNP, (b) Ni(OH) ₂ /GNP, (c) CeO ₂ /GNP, (d) commercial 20 wt% Pt/C, and (e) GNP in N ₂ - and O ₂ -saturated 0.1M KOH and scan rate 10 mV s ⁻¹ .	3-8
3A.8	LSVs of (a) Co ₃ O ₄ /GNP, (b) Ni(OH) ₂ /GNP, (c) CeO ₂ /GNP, (d) commercial 20 wt.% Pt/C, and (e) GNP in O ₂ -saturated 0.1M KOH at different scan rates from 400–3600 rpm and scan rate 10 mV s ⁻¹ .	3-9
3A.9	(a) LSVs in O ₂ -saturated 0.1M KOH at 1600 rpm and scan rates 10 mV s ⁻¹ , and (b) Mass specific activities of the catalysts.	3-10
3A.10	(a–c) CVs of the as-synthesized catalysts at different scan rates from 10–60 mV s ⁻¹ , and (d–f) Double layer capacitance (C _{DL}) derived from slope of charging current vs. scan rates.	3-11
3A.11	(a–c) K-L plots of Co ₃ O ₄ /GNP, Ni(OH) ₂ /GNP and CeO ₂ /GNP at potentials 0.5 V, 0.6 V and 0.7 V, and (d) Bar diagram showing number of electrons (n) transferred in ORR process.	3-12
3A.12	LSVs at 1600 rpm of (a) Co ₃ O ₄ /GNP, (b) Ni(OH) ₂ /GNP, (c) CeO ₂ /GNP, and (d) commercial 20 wt.% Pt/C in O ₂ -saturated 0.1M KOH before and after 10,000 cycles.	3-13
3A.13	Bar diagram showing E _{1/2} before and after ADT (left	3-13

	axis) and their shifts in $E_{1/2}$ (right axis).	
3A.14	CA test at 1600 rpm for the catalysts at 0.5V for 5.5 h.	3-14
3A.15	(a) LSVs in N_2 -saturated 0.1M KOH at 1600 rpm and scan rates 10 mV s^{-1} , and (b) Overpotentials of the catalysts for OER.	3-14
3B.1	PXRD of (a) $Co_3O_4/CeO_2/GNP$, (b) $Ni(OH)_2/CeO_2/GNP$, and (c) $CoNiCe/GNP$.	3-16
3B.2	FTIR spectra of (a) $Ni(OH)_2/CeO_2/GNP$, (b) $Co_3O_4/CeO_2/GNP$, and (c) $CoNiCe/GNP$.	3-17
3B.3	(a) Raman spectra, and (b) TGA of the as-synthesized catalysts.	3-18
3B.4	EDX analysis of $Co_3O_4/CeO_2/GNP$; (a) the electron image (b) the EDX pattern, and (c–f) elemental maps for individual Co, Ce, O and C, respectively.	3-19
3B.5	EDX analysis of $Ni(OH)_2/CeO_2/GNP$; (a) the electron image (b) the EDX pattern, and (c–f) elemental maps for individual Ni, Ce, O and C, respectively.	3-19
3B.6	EDX analysis of $CoNiCe/GNP$; (a) the electron image (b) the EDX pattern, and (c– g) elemental maps for individual Ni, Co, Ce, O and C, respectively.	3-20
3B.7	(a,b,c) Low-resolution TEM images, (d) SAED pattern, (e) high-resolution TEM (HRTEM) image, and (f– g) FFT images of the marked regions in (e) of $Co_3O_4/CeO_2/GNP$.	3-20
3B.8	(a,b) Low-resolution TEM images, (c,d) SAED patterns, (e,f) high-resolution TEM (HRTEM) images, and (g–j) FFT images of the marked regions in (f) of $Ni(OH)_2/CeO_2/GNP$.	3-21
3B.9	(a) Low-resolution TEM images, (b) high-resolution TEM (HRTEM) image (c), SAED pattern, (d) HRTEM image at a different resolution, and (e–j) FFT images of the marked regions in (d) of $CoNiCe/GNP$. From the FFT images, most observed fringes are crystallites of	3-22

CeO₂ while the other components, viz. Ni(OH)₂, Co₃O₄ and CeO₂ are amorphous.

3B.10	(a–c) CVs of Co ₃ O ₄ /CeO ₂ /GNP (a), Ni(OH) ₂ /CeO ₂ /GNP (b), and CoNiCe/GNP (c) in N ₂ - and O ₂ -saturated) in 0.1M KOH , and (d–e) LSVs of Co ₃ O ₄ /CeO ₂ /GNP (d), Ni(OH) ₂ /CeO ₂ /GNP (e), and CoNiCe/GNP (f) at different rotation rates from 400–3600 rpm.	3-23
3B.11	(a) LSV@1600 rpm for ORR, and (b) Bar diagram representing mass specific activities calculated at 0.4 V.	3-23
3B.12	(a–c) CVs of the catalysts at different scan rates, and (d) Double layer capacitance (C _{DL}) derived from slope of charging current of the CVs.	3-24
3B.13	Bar diagram representing mass specific ECSAs.	3-25
3B.14	(a– c) K-L plots of Co ₃ O ₄ /CeO ₂ /GNP (a), Ni(OH) ₂ /CeO ₂ /GNP (b), CoNiCe/GNP (c) in the potential window 0.5– 0.7 V, and (d) Bar diagram representing number of electrons transferred ‘n’ during ORR.	3-26
3B.15	ADT of (a) Co ₃ O ₄ /CeO ₂ /GNP, (b) Ni(OH) ₂ /CeO ₂ /GNP, (c) CoNiCe/GNP, and (d) 20 wt.% Pt/C.	3-27
3B.16	CA test at 0.5 V of the as-synthesized catalysts and commercial 20 wt.% Pt/C.	3-27
3B.17	(a) LSV@1600 rpm for OER, (b) Bar diagram representing overpotentials, and (c) Diagram showing bifunctionality index of Co ₃ O ₄ /CeO ₂ /GNP.	3-28
4.1	PXRD spectra of (a) Co ₃ O ₄ /GNP, (b) CeO ₂ /GNP, and (c) Co ₃ O ₄ /CeO ₂ /GNP.	4-3
4.2	(a) FTIR spectra, (b) Raman spectra, (c) N ₂ adsorption/desorption isotherms with BJH pore distribution (inset), and (d) TGA of various catalysts.	4-4
4.3	EDX-elemental mapping of the atoms C, O, Co and Ce for the catalyst Co ₃ O ₄ /CeO ₂ /GNP for two electron images (a,c) with the composition tables shown in insets,	4-7

	(b,d) corresponding spectra from elemental mappings. The elemental maps are shown in insets of (b,d).	
4.4	(a) HR-TEM image of $\text{Co}_3\text{O}_4/\text{CeO}_2/\text{GNP}$ showing loosely bound aggregates on graphene sheets (b) Histogram for particle size distribution (c) SAED pattern with concentric rings indexed to corresponding Miller planes (d) low resolution TEM image used to determine particle size distribution and (e) HR-TEM image showing different crystallites of Co_3O_4 and CeO_2 with lattice fringes indexed in (f).	4-8
4.5	(a) Core O 1s XP spectra, and (b) bar diagram representing %composition of O_{ads} , O_{v} and O_{lat} in the as-synthesized catalysts.	4-9
4.6	(a) Wide range survey spectrum, (b) C 1s XP spectrum, (c) Co 2p XP spectrum, and (d) Ce 3d XP spectrum of $\text{Co}_3\text{O}_4/\text{CeO}_2/\text{GNP}$.	4-11
4.7	(a) Wide range survey spectrum, (b) C 1s spectra, and (c) Co 2p core spectra of $\text{Co}_3\text{O}_4/\text{GNP}$.	4-11
4.8	(a) Wide range survey spectrum, (b) C 1s spectra and (c) Ce 3d core spectra of CeO_2/GNP .	4-12
4.9	(a) Cellulose supported pellets on pellet rack for ex-situ XAS studies on B18 beamline at Diamond Light Source synchrotron facilities, (b) XAS of $\text{Co}_3\text{O}_4/\text{CeO}_2/\text{GNP}$ and $\text{Co}_3\text{O}_4/\text{GNP}$ with EXAFS region marked.	4-13
4.10	(a) Overlay of XANES of three standards— Co, CoO, Co_3O_4 and the as-synthesized catalysts $\text{Co}_3\text{O}_4/\text{CeO}_2/\text{GNP}$ and $\text{Co}_3\text{O}_4/\text{GNP}$ (b) white line region and (c) pre-edge region of $\text{Co}_3\text{O}_4/\text{CeO}_2/\text{GNP}$ and $\text{Co}_3\text{O}_4/\text{GNP}$ (d) k^2 -weighted Fourier transform of Co K-edge EXAFS and their 1 st shell fits obtained with $R = 1.2\text{--}3.4 \text{ \AA}$ (e) Linear plot of edge energy vs. oxidation states.	4-14
4.11	CVs of as-synthesized $\text{Co}_3\text{O}_4/\text{CeO}_2/\text{GNP}$, $\text{Co}_3\text{O}_4/\text{GNP}$	4-16

	and CeO ₂ /GNP under N ₂ and O ₂ -saturated 0.1 M KOH at scan rate 10 mV s ⁻¹ .	
4.12	LSVs of (a) Co ₃ O ₄ /CeO ₂ /GNP, (b) Co ₃ O ₄ /GNP, and (c) CeO ₂ /GNP in O ₂ -saturated 0.1M KOH at 10 mV s ⁻¹ .	4-16
4.13	(a,c) CVs of Pt/C and GNP, and (b,d) LSVs of Pt/C and GNP, at 10 mV s ⁻¹ .	4-17
4.14	(a) LSVs of the catalysts at 1600 rpm with their current densities at 0.2 V, 0.4 V and 0.6 V marked, (b) Bar diagram representing current densities at 0.2 V, 0.4 V and 0.6V, (c) Bar diagram representing mass specific activities at 0.6V, and (d) Plot of $(i \times i_L)/(i_L - i)$ vs. E. Potentials for each catalyst to reach the target i_k are marked.	4-18
4.15	(a–c) CVs of the as-synthesized catalysts at different scan rates from 10–60 mV s ⁻¹ , and (d–e) Double layer capacitances (C _{DL}) derived from slope of charging current of the CVs.	4-19
4.16	Bar diagram showing mass specific ECSAs.	4-20
4.17	K-L plots for (a) Co ₃ O ₄ /CeO ₂ /GNP, (b) Co ₃ O ₄ /GNP, (c) CeO ₂ /GNP, (d) GNP and (e) number of electrons (n) transferred in ORR in different potentials.	4-21
4.18	(a) LSVs of Co ₃ O ₄ /CeO ₂ /GNP before and after 10,000 CV cycles, (b) CA for current retention of Co ₃ O ₄ /CeO ₂ /GNP at potential 0.67 V vs. RHE, (c) LSVs of commercial standard RuO ₂ and the as-synthesized catalysts Co ₃ O ₄ /CeO ₂ /GNP, Co ₃ O ₄ /GNP and CeO ₂ /GNP at 1600 rpm towards OER, and (e) bifunctionality index of Co ₃ O ₄ /CeO ₂ /GNP.	4-22
5.1	PXRD spectra of the as-synthesized catalysts.	5-4
5.2	(a) FTIR spectra (b)TGA curve in air atmosphere.	5-5
5.3	(a) Raman spectra showing I _D /I _G values, and (b) Raman spectra showing vibrational modes and shifts in F _{2g} peak in Co ₃ O ₄ /Co _x Ce _{1-x} O _{2-δ} /C.	5-6

5.4	(a) TEM images of $\text{Co}_3\text{O}_4/\text{Co}_x\text{Ce}_{1-x}\text{O}_{2-\delta}/\text{C}$ (b) SAED pattern with rings indexed to appropriate Miller planes (c,d) HR-TEM images showing lattice fringes and interplanar spacing (e-g) inverse FFTs of depicted areas in (c).	5-7
5.5	(a) XPS survey spectra, and (b) O 1s core XP spectra with $\text{O}_\text{S}/\text{O}_\text{L}$ ratios and %composition of O_V mentioned of the as-synthesized catalysts.	5-9
5.6	Co 2p core XP spectra of $\text{Co}_3\text{O}_4/\text{Co}_x\text{Ce}_{1-x}\text{O}_{2-\delta}/\text{C}$, $\text{Co}_3\text{O}_4/\text{C}$ and CeO_2/C .	5-10
5.7	Ce 3d core XP spectra of $\text{Co}_3\text{O}_4/\text{Co}_x\text{Ce}_{1-x}\text{O}_{2-\delta}/\text{C}$ and CeO_2/C .	5-11
5.8	CVs of (a) as-synthesized catalysts, (b) graphene nanoplatelets, and (c) commercial 20 wt% Pt/C, in N_2 - and O_2 -saturated 0.1M KOH at scan rate 10 mV s^{-1} .	5-12
5.9	LSVs of (a–c) the as-synthesized catalysts, (d) of graphene nanoplatelets (C), and (e) of commercial 20 wt.% Pt/C, in O_2 -saturated 0.1M KOH at scan rate 10 mV s^{-1} .	5-12
5.10	(a) A comparative overlay of LSV@1600 rpm of the studied catalysts in O_2 -saturated 0.1M KOH; scan rate 10 mVs^{-1} , and (b) Bar diagram of mass specific activities of the catalysts calculated at 0.4 V.	5-13
5.11	(a–c) CVs of the as-synthesized catalysts at different scan rates from $10\text{--}60 \text{ mV s}^{-1}$, and (d–e) Double layer capacitance (C_{DL}) derived from slope of charging current of the CVs.	5-14
5.12	K-L plots and derived number of electrons (n) at 0.4 V.	5-15
5.13	LSVs@1600 rpm before and after 10,000 cycles for (a) Pt/C, and (b) $\text{Co}_3\text{O}_4/\text{Co}_x\text{Ce}_{1-x}\text{O}_{2-\delta}/\text{C}$ and their shift of $E_{1/2}$.	5-15
5.14	Results of 6 h CA test at 0.5 V with their relative current retention.	5-16

5.15	(a) LSV@1600 rpm towards OER along with RuO ₂ , (b) Bar diagram showing the overpotential@10 mA cm ⁻² , and (c) Diagram showing bifunctionality index of Co ₃ O ₄ /Co _x Ce _{1-x} O _{2-δ} /C towards ORR and OER.	5-17
6.1	PXRD of CoO _x (OH) _y /C and the Co/Ce/C hybrids with JCPDS indexes.	6-3
6.2	(a) FTIR spectra, and (b) Raman spectra of the catalysts with functional groups and vibrational modes indexed.	6-4
6.3	TEM images of CoO _x (OH) _y /C and the CoO _x (OH) _y /CeO ₂ /C (1:1, 3:1 and 9:1) hybrids.	6-6
6.4	FESEM images of freshly drop-casted electrodes and used electrodes of (a) Co/Ce/C-1:1, (b) Co/Ce/C-3:1 and (c) Co/Ce/C-9:1.	6-6
6.5	XPS survey spectrum of the Co/Ce/C hybrids.	6-7
6.6	Core XP spectra of the Co/Ce/C hybrids for (a) Co 2p, (b) Ce 3d, (c) O 1s and (d) Bar diagram representing %composition of Co ^{2+/3+} ions and Co ²⁺ /Co ³⁺ ratio.	6-9
6.7	EPR spectra of CoO _x (OH) _y /C and Co/Ce/C hybrids (a) overlay view for intensity comparison, and (b) stacked view for better visual observation.	6-10
6.8	XANES spectra of the as-synthesized catalysts CoO _x (OH) _y /C, the Co/Ce/C hybrids, and three standards—Co foil, CoO, Co ₃ O ₄ .	6-11
6.9	CVs of the catalysts in (a) N ₂ -saturated and (b) O ₂ -saturated 0.1M KOH at scan rate 10 mV s ⁻¹ .	6-13
6.10	LSVs of the catalysts at different rotation rates from 400–3600 rpm for the Co/Ce/C hybrids (a) Co/Ce/C-1:1, (b) Co/Ce/C-3:1, (c) Co/Ce/C-9:1, (d) CoO _x (OH) _y /C, and (e) CeO ₂ /C.	6-13
6.11	(a) LSVs of the catalysts and commercial Pt/C at 1600 rpm, and (b) bar diagram representing mass specific activities at 0.5V.	6-14
6.12	Scan rate dependent CVs of (a) CoO _x (OH) _y /C, (b)	6-15

	CeO ₂ /C, (c) Co/Ce/C-1:1 (d) Co/Ce/C-3:1, and (e) Co/Ce/C-9:1.	
6.13	(a) Current vs. Scan rate plots with slope C _{DL} , and (b) bar diagram representing mass specific ECSA of the catalysts.	6-16
6.14	Koutecky-Levich (K-L) plots of (a) CoO _x (OH) _y /C, (b) Co/Ce/C-1:1, (c) Co/Ce/C-3:1, (d) Co/Ce/C-9:1, and (e) CeO ₂ /C.	6-17
6.15	Average number of electrons transferred in potential range 0.55–0.7 V.	6-18
6.16	LSVs of the as-synthesized catalysts (a) CoO _x (OH) _y /C, (b) Co/Ce/C-1:1, (c) Co/Ce/C-3:1, (d) Co/Ce/C-9:1, and (e) commercial 20 wt.% Pt/C before and after 10,000 CVs.	6-19
6.17	Bar diagram consisting of half-wave potentials (E _{1/2}) before and after ADT test and the corresponding shifts in E _{1/2} are shown by line diagram.	6-20
6.18	(a) Chronoamperometry (CA) test results of CoO _x (OH) _y /CeO ₂ 3:1 and commercial 20 wt% Pt/C conducted at 0.4 V, and (b) Bar diagram representing the % current retention of CA test.	6-20
6.19	(a) RDE-LSVs of the as-synthesized catalysts at 1600 rpm for OER in N ₂ -saturated 0.1M KOH and scan rate 10 mV s ⁻¹ . The dotted line represents the current density of 10 mA cm ⁻² . (b) Bar diagram representing the overpotentials.	6-21
7.1	Schematic summary of chapter-wise experimental findings.	7-5
7.2	A bar diagram comprising of the best catalyst from each chapter and their catalytic performance indicators.	7-7